

Charcoal and fly-ash particles from Lake Lucerne sediments (Central Switzerland) characterized by image analysis: anthropologic, stratigraphic and environmental implications

Florian Thevenon*, Flavio S. Anselmetti¹

Geological Institute, ETH Zurich, 8092 Zurich, Switzerland

Received 30 August 2006; received in revised form 24 May 2007; accepted 31 May 2007

Abstract

In order to link the charcoal record from sedimentary archives with the combustion processes that reflect past anthropogenic activity, a novel method based on automated image analysis was developed. It allows a detailed quantification and morphological analysis of the combustion-derived products that were emitted in the area of Lake Lucerne (Central Europe) throughout the last 7200 years.

Charcoal-particle distribution reconstructed from the composite sedimentary record shows that the charcoal input is primarily linked to redistribution of detrital μm -size charcoal degradation products from surface runoff into the large lake basin. However, the independent distribution of the coarser charcoal fraction ($> 38 \mu\text{m}$) exhibits four major periods of large-scale fire activity around 5500, 3300, 2400, and 530 cal. BP. These events are synchronous with major anthropogenic changes (lake-dwellings, land-use changes, technological innovations), although it is possible that these major fire episodes could have been indirectly triggered by climatic deterioration and unfavorable environmental conditions. During the late-nineteenth-century, a great increase in slag particles and magnetic spherules of fly-ash occurred due to the steamboat navigation on Lake Lucerne. The successive burning of wood (after AD 1838), coal (after AD 1862), and diesel (after AD 1931) by the steamboat traffic produced specific particle shapes, providing valuable chronological markers for dating the recent sediments and a proxy for fossil fuel combustion.

© 2007 Elsevier Ltd. All rights reserved.

1. Introduction

The intercomparative analysis of charred particles from different paleoclimatic archives (i.e. lake, ocean, peat, and ice deposits) is an important but challenging task for reconstructing the major disturbances caused by fire, the dynamics of the pyrogenic carbon cycle, and recent human impact on the emissions of atmospheric pollutants. Although an important effort has been undertaken in the last decade, in order to improve the chemical quantification of the micrometric and most refractory black carbon (BC) fractions (Currie et al., 2002), optical microscope measurements still lack any standardized method (Turner et al., in press). This is highly surprising, because (1) the coarse and

slightly charred biomass components determined by microscopic charcoal techniques cannot be recovered by the BC chemical approaches, but nevertheless constitute the vast majority of the fire-derived carbon from biomass combustion (Thevenon et al., in press), and (2) new developments in computer technology have been recently applied to sedimentological and paleoenvironmental studies (Francus et al., 2004), allowing high-resolution quantitative and qualitative particle analyses through image-processing techniques (Seelos and Sirocko, 2005; Gälman et al., 2006).

There are several reasons for the interest in measuring precisely the charcoal trapped in sedimentary deposits as a separate paleoenvironmental proxy (Turner et al., in press). First, the charcoal particles contribute strongly to the slow cycling carbon pools in soils and sediments (Andreae, 1991) and represent a significant sink for the fast atmospheric–biospheric carbon cycle (Kuhlbusch and Crutzen, 1995). However, in order to ensure comparative data

*Corresponding author. Tel.: +41 44 632 80 63; fax: +41 44 6332 10 75.
E-mail address: Florian.Thevenon@yahoo.fr (F. Thevenon).

¹Present address: Eawag, Swiss Federal Institute of Aquatic Science and Technology, CH-8600 Dübendorf, Switzerland.

synthesis, the charcoal particle quantification from different analytical techniques and scientific approaches should be reproducible with precise experimental parameters, allowing a calibration using geochemical standards of accurately known carbon composition. Second, the majority of the conventional charcoal-stratigraphic studies generally focus on sediment cores from small lakes, counting particles $>10\ \mu\text{m}$ and/or $>100\text{--}200\ \mu\text{m}$ (Clark et al., 1996; Carcaillet et al., 2002), while particles smaller than $2\ \mu\text{m}$ that make up more than 80% of the airborne combustion products (Suman et al., 1997) are not detected. Consequently, conventional microscopic charcoal analysis, which does not pick up any soot carbon and sub- μm charcoal degradation products, cannot be applied to paleoclimatic archives for quantifying the sub- μm size particle signal. In addition, by focusing on the window of the combustion continuum with a short paleotracer range (Masiello, 2004), conventional sedimentary charcoal time series record the burning history of local ecosystems (Clark and Patterson, 1997; Tinner et al., 2006) but provide no direct information about the signal from smaller and refractory charred particles (e.g. reburial of fossil sub- μm particles, remote fire activity, or fires of low severity; Higuera et al., 2005). Furthermore, charcoals are commonly detected by visual criteria, which can vary from one user to another, or be modified by the different extraction (e.g. chemical and mechanical treatments) and quantification procedures (e.g. bleaching and filtering, density separation, light-intensity of the microscope, etc.) that finally induces large variations in the amount of charcoal recorded (Turner et al., *in press*). Last but not the least, the manual counting of the smallest size fragments, which can account for thousands of particles per field of view, as well as the manual measurements of the largest charcoal morphologies is time consuming and tedious, even for a trained human expert.

Variability in particle shape of the combustion-derived products can provide useful information about the associated operating parameters of combustion processes or the combustible material burnt (Umbanhowar and McGrath, 1998; Thevenon et al., 2003). The high-temperature combustion of oil and coal, for example, produces specific spheroidal carbonaceous particles (SCPs) and inorganic ash spheres (IASs) that can be counted and compared with historic records of fossil-fuel combustion, to provide valuable chronologic markers for dating the recent sediment cores (Rose et al., 1995; Kralovec et al., 2002). To our knowledge, however, there is no study in which fly-ash particles have been estimated automatically, and no fly-ash particle profile is available from Swiss lake sediments. The primary objective of this study is therefore to characterize with a reproducible automated image analysis technique, the charred carbon deposited in a large European lake throughout the mid-late Holocene period. The inferred biomass burning activity record can be then compared with available archaeological, historic, and climatic data. A further objective of this research is to

decipher the presence of chronostratigraphic markers for dating the nineteenth-century sediments of Lake Lucerne. To achieve these goals, an automated image-processing technique has been developed and applied to Lake Lucerne sediment samples, in order to digitize the grey-scale variations of the binary images that are obtained by scanning the samples, and to measure the area and morphology of the dark particles remaining after thresholding the grey-level of the images.

2. General setting and strategy

2.1. Lake Lucerne

Lake Lucerne is a perialpine lake located in Central Switzerland (47°N , 8°E ; 434 m a.s.l.) at the northern alpine front (Fig. 1a). With an area of $116\ \text{km}^2$, Lake Lucerne is far larger than those lakes normally used for the reconstruction of fire histories (ca $0.1\text{--}0.3\ \text{km}^2$; Tinner et al., 1999; Carcaillet, 2007). Despite the presence of steep-sided basins and inflowing streams that could transport secondary charcoal, the lake possesses many attributes that makes its sedimentary archive a strong candidate for studying biomass burning and fossil-fuel combustion products: While four internal basins of Lake Lucerne are fed by four major alpine rivers (Reuss, Muota, Engelberger Aa and Sarner Aa; Fig. 1b) providing $\sim 80\%$ of the lakes total water supply ($109\ \text{m}^3/\text{s}$), three external basins, separated by sub-lacustrine sills formed by the glacial erosion and moraine deposits (forming narrow passageways; Fig. 1b) are relatively isolated from coarse terrestrial clastic contributions. As a consequence, these external basins contain a hemipelagic record that lacks significant redistribution of fossil and refractory organic matter, which generally overprints and biases the fire record. Moreover, the large catchment area of Lake Lucerne ($2124\ \text{km}^2$) delivers charcoals from wide areas to be collected and deposited into the lacustrine sediments. This point is crucial for recording large-scale signals of biomass burning activity and for apprehending the charred carbon stored in such a large lake.

2.2. Coring site

Long piston cores have been retrieved and studied from Lake Lucerne, along with seismic profiles within a study of the Limnogeology Laboratory at the ETH, Zurich that investigated mass-movement processes and reconstructed the prehistoric mass-movement and earthquake history (Schnellmann, 2004, Fig. 1c). This previous work allowed us to select an ideal site with a continuous sedimentary record, avoiding the influence of large mass-movement deposits (Fig. 1c and Section 4.1). Furthermore, the coring site was chosen on the boat trajectory towards the port of Lucerne, so that recent sediments may provide information about the emission of combustion products related to the steamboat navigation during the nineteenth- and twentieth-century.

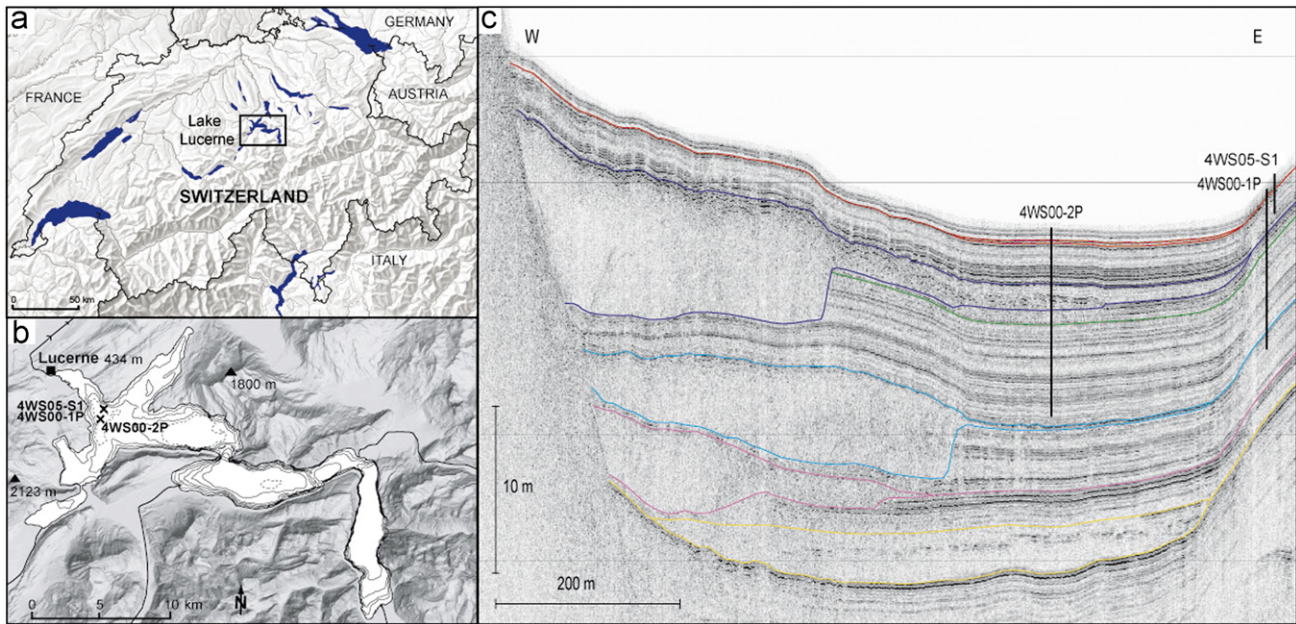


Fig. 1. (a) Map of Switzerland with the largest Swiss lakes indicated. (b) Bathymetric and topographic map of Lake Lucerne showing the location of the city of Lucerne situated on the outflow River Reuss, cores 4WS05-S1, 4WS00-1P, and 4WS00-2P (bathymetric contour interval is 40 m). (c) Seismic profile across Chrüztrichter Basin of Lake Lucerne showing the core locations and the mass flow deposits and megaturbidites (modified from Schnellmann, 2004).

Here, we use the existing data and material, as well as one additional short core, to study the sedimentary record and the pyrogenic products therein together with their environmental implications at high-resolution. Both cores were taken at the same location ($47^{\circ}03'04''\text{N}$, $8^{\circ}35'26''\text{E}$) in 110 m water depth just a few meters above the basin floor on the lower slope of a subaquatic hill in the middle of the the Chrüztrichter Basin (Fig. 1). The long piston core (4WS00-1P, 8.6 m length; collected in 2000) and the short core (4WS05-S1, 1.8 m length; collected in 2005) contain both a specific black and sandy layer standing out prominently in core photographs and granulometry profile (at 163–166 cm in the short core and at 173–180 cm in the long core, respectively; Figs. 2 and 3). This horizon allows an accurate core-to-core correlation so that a 5.5 m long continuous composite section can be defined, consisting of the top of the short core and of the bottom of the long piston core (Figs. 2 and 3).

2.3. Regional history and relevant microscopic chronostratigraphic makers

During the Middle Age, Lake Lucerne became an important link in trade between northern Europe and the Mediterranean coast, especially after the opening of the Gotthard Pass around AD 1230. This pass was the shortest route from north to south across the Alps, and the north end of this road was at the southern tip of Lake Lucerne. However, the inneralpine inflow (Reuss delta) could only be reached from the outflow of the lake in Lucerne by boat, because steep cliffs prevented early construction of a connecting lake shore road. When the Gotthard road was

built in AD 1830, freight and passenger commerce on Lake Lucerne increased rapidly. Travelers could travel from the end of the boat trip across the Alps right down to the Italian border. Once the entire lake was opened for steam navigation, several steamboat companies formed and tourism rapidly developed. These first steamboats (AD 1838) were wood burners until AD 1862, when they began to burn coal. The activity of the steamship lines was reduced during world wars, in between which the coal-heated paddle steamers were overhauled and transformed into oil-fired ships since AD 1931 in the context of the development of the diesel motor boat. In such a context, we expect to find different particle morphologies in the recent sediments that mark the advent of wood, coal, and oil burning by the steamboats, so that we can refine age estimates of the recent deposits that are not datable with the radiocarbon method. These microscopic stratigraphic markers are outlined in Table 1 in the order of their occurrences.

3. Methods

3.1. Sample preparation

Gamma-ray attenuation (bulk density) and magnetic susceptibility were first measured with a GEOTEKTM multisensor core-logger with a resolution of 0.5 cm. The sampling resolution for charcoal analysis ranges from 1 cm (between 1 and 25 cm down-core), to 1–2 cm (between 25 and 177 cm down-core), and 3–5 cm (between 177 and 575 cm down-core). In order to optimize time and expenses, we combined the charcoal extraction with the

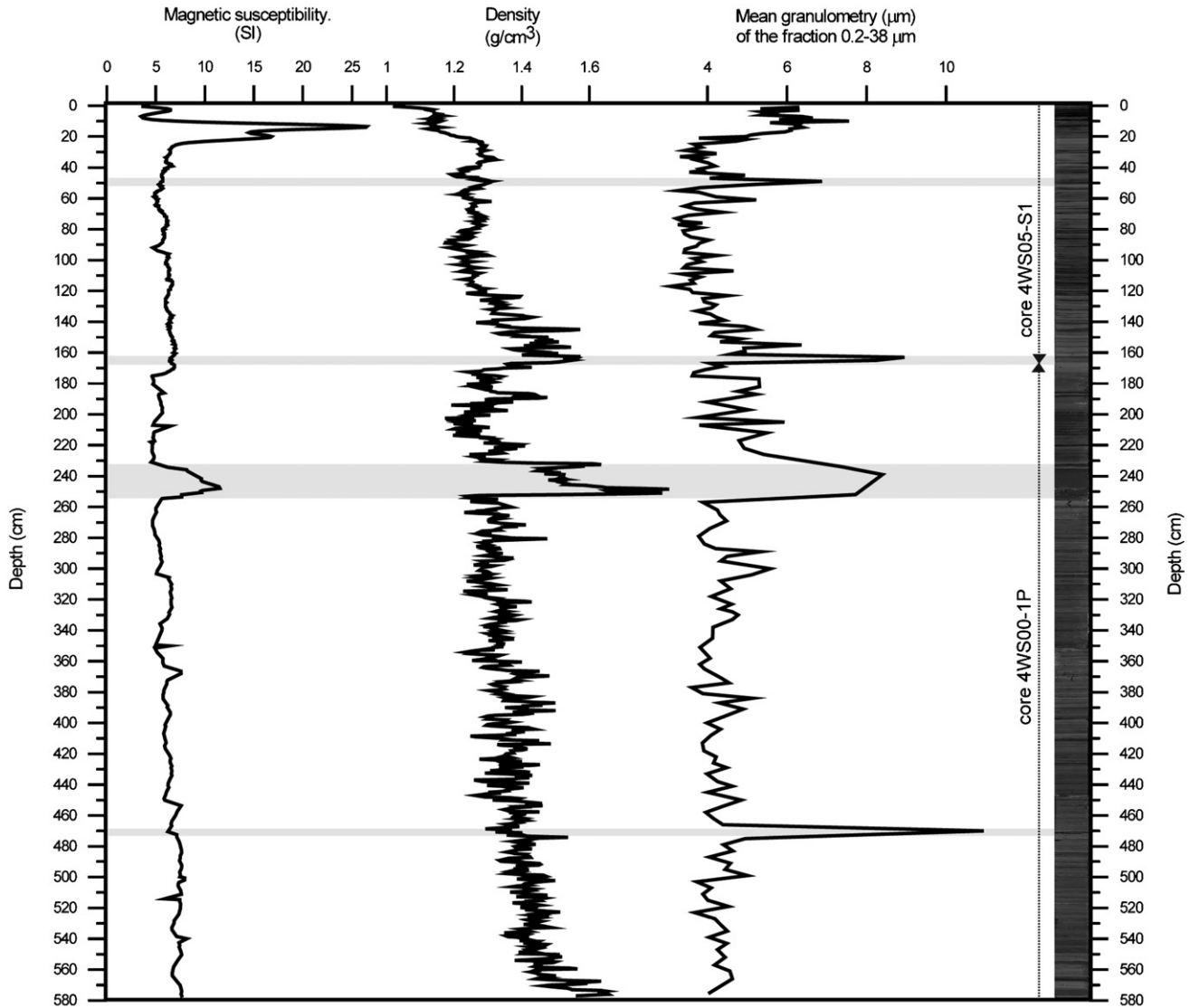


Fig. 2. Composite sedimentary section with measurements of magnetic susceptibility, gamma-ray attenuation bulk density, mean granulometry and core photographs for cores 4WS05-S1 and 4WS00-1P. Shaded areas indicate the silty turbidites that were removed from the composite sedimentary record for age model and analysis and interpretation of pyrogenic products.

preparation of the samples for the granulometry analysis. The method follows the one described in Thevenon et al. (2003, 2004), which involves the removal of labile organic matter and carbonates.

About 0.2–0.5 g of dried and non-crushed sediment was set in a 250 ml glass beaker. The sediment was dispersed in ultrasonic water-sound for 5 min using 20 ml sodium pyrophosphate ($\text{Na}_4\text{O}_7\text{P}_2$) as a deflocculant for clays. 20 ml hydrochloric acid (3 M HCl) was added into the beaker for 24 h to remove carbonates. To remove the labile organic fraction, 20 ml concentrated nitric acid for 24 h and 40 ml of hydrogen peroxide (33% H_2O_2) for 48 h, were successively added into the beaker.

Then the solution was gently screened through a 38 μm sieve collecting the liquid. The residue $> 38 \mu\text{m}$ was isolated on a nitrocellulose filter (47 mm diameter, 0.22 μm porosity), which was placed in Petri dish for observation using

the incident-light microscope. 10 ml of the fraction $< 38 \mu\text{m}$ were isolated on a nitrocellulose filter. A part of this filter was mounted onto a microscope slide with Canadian balsam for observation using the transmitted-light microscope. About 100 ml of the solutions were filtered on a nitrocellulose filter and stored in Petri dish for the grain size analysis.

3.2. $> 38 \mu\text{m}$ black particles analysis by the automated incident-light microscope

The automated incident-light microscope is equipped with a simple black and white TV CCD video camera that is connected to a video frame grabber. Processing of 256 grey-scale pictures produces binary (black and white) images, on which each of the pixels represents a grey-scale value ranging from 0 (white) to 255 (black). The pixel

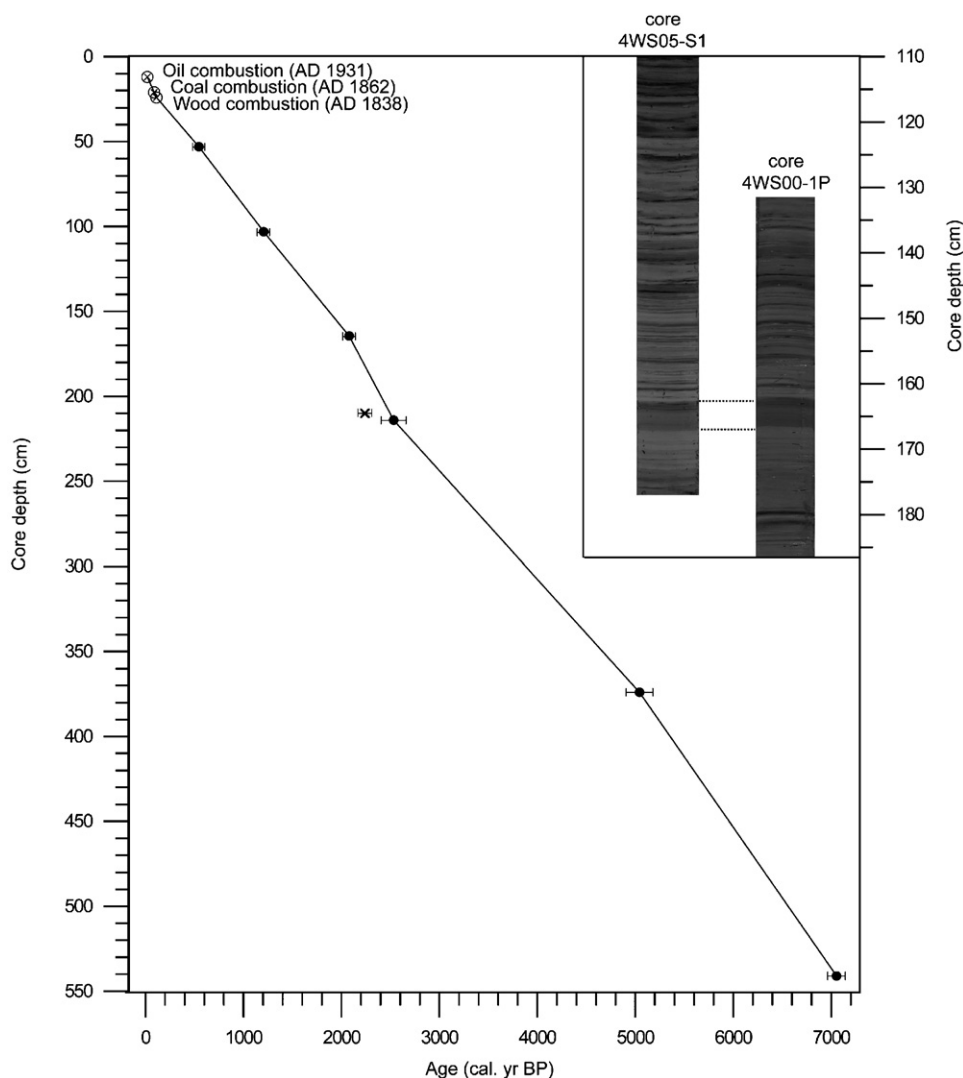


Fig. 3. Age model of the composite sedimentary section, established using appearance of combustion products (as stratigraphic markers) and radiocarbon age dates from cores 4WS05-S1 and 4WS00-P1. The cross indicates alternate ^{14}C date from nearby core 4WS00-P2 (Schnellmann et al., 2006; see discussion). Core photographs show the stratigraphic tie-point of the core-to-core correlation, where the composite section jumps from the short core (above) to the long piston core (below).

Table 1
Pyrogenic microscopic products, as potential chronostratigraphic markers for Lake Lucerne sediments

Year AD	Event	Predictive stratigraphic marker
1931	Replacement of the steamboat by diesel motor boats	Increase in oil-based particles
1862	Initiation of coal-fueled steamboats	Increase in coal-based particles
1838	Beginning of wood-fueled steamboat activity	Increase in wood-based particles

resolution of the grabbed images (768×576 pixels) provides a pixel size of $1.38 \mu\text{m}$ at maximum magnification. For each sample, the entire surface of the filter (ca 17cm^2) was automatically scanned by the incident-light micro-

scope. About 2000 images were captured with a video frame grabber (ca 70 min/filter), and analysed using the *analySIS*[®] 5 software package (Soft Imaging System GmbH, Germany). A rapid overview of the images was performed before the analysis, in order to check the quality of the images (mainly depending on the presence of non-charcoal opaque minerals) and to remove manually any dubious images. The grey-value threshold for the quantification of the combustion-derived products was fixed at the level of 165. The area, diameter, and sphericity measurements were calculated for each detected charcoal particle. Finally, the black particles having a sphericity >0.9 (a sphericity of 1 is a circular particle) were defined as spherical fly-ash particles. The goal of such approach was not to quantify the fly-ash particles in an exhaustive way, but to use the available morphological parameters of the black particles $>38 \mu\text{m}$ to locate accurately the occurrence of the fossil fuel combustion products in the record.

Despite the fact that the majority of the fly-ash particles may have smaller diameters (Odgaard, 1994; Wik and Renberg, 1996), the spherical fly-ash particles $<38\ \mu\text{m}$ were not identified in this study.

3.3. $<38\ \mu\text{m}$ charcoal analysis by the automated transmitted-light microscope

The automated transmitted-light microscope system is equipped with a highly sensitive black and white slow scan camera that is connected to a video frame grabber. The pixel resolution of the grabbed images (1600×1200 pixels) provides a pixel size of $0.16\ \mu\text{m}$ at maximum magnification. About 200 fields of view (ca $10\ \text{mm}^2$) were automatically acquired (ca 20 min) from each smear-slide. A rapid overview of the images was achieved to control the quality of the images (mainly depending on the microscope autofocus and the presence of oxidant resistant organic material) and to erase by hand any spurious images. Images were eventually analysed using Image/J software (Rasband, WS, Image J, NIH, Bethesda, MD, USA). The combustion-derived products were isolated by thresholding the grey-level of the images at the value of 200.

3.4. Laser granulometry

About 20–50 mg of the screened sediment ($0.22\text{--}38\ \mu\text{m}$) was placed into a beaker for ultrasonic dispersion during 5 min. Grain size analysis was carried out using a *MasterSizer* laser-optical grain size analyzer from *Malvern Instrument Inc.* The *MasterSizer* provides a size distribution by volume of equivalent spheres, and the grain size analysis results are reported as the mean over the volume distribution for representing the grain size distribution.

4. Results

4.1. Sedimentological and petrophysical features

Whereas the values of the magnetic susceptibility are relatively stable for the lower part of the core (except in the silty horizons, see next section), the recent sediments exhibit an abrupt increase in magnetic mineral concentration between 24 and 11 cm (Fig. 2). This rise in magnetic susceptibility is, however, accompanied by a decrease in density (Fig. 2). Considering that the inorganic minerals present in fossil-fuel include iron-rich components, pyrite may transform to hematite and magnetite upon fossil-fuel combustion, leading to the formation of slag particles and magnetic spherules of fly-ash (Goldberg et al., 1981). Therefore, and because no major sedimentary change can be seen in the sedimentological description, the recent sharp and short increase in magnetic mineral concentration may reflect the historic emissions linked to coal-powered vessels. This hypothesis is confirmed by the simultaneous increase in the influx of spherical fly-ash particles (Fig. 5) which are likely iron-rich inorganic ash spheres derived

from coal combustion. Such a result is an interesting and important aspect for dating the recent sediment-cores, as a similar magnetic signal could be used for dating some sedimentary records from other large Swiss lakes, bridging the dating gap between $^{137}\text{Cs}/^{210}\text{Pb}$ and ^{14}C methods.

The density and granulometry profiles show, with different resolution, a roughly similar pattern throughout the record (Fig. 2). Without considering the granulometry increase in the recent sediments (above 24 cm), four major coarser-grained turbidites occur in the composite section. The grain size profile and the core photographs have been used to precisely identify these silty layers, at 51–49, 166–163, 252–234, and 471–470 cm (Fig. 2). These horizons likely correspond to four mass flow events that affected this part of the Chrüztrichter basin and that were described by Schnellmann et al. (2006). Because these four turbidites were abruptly deposited and possibly contain redistributed material (Strasser et al., 2007; Girardclos et al., 2007), they have been subtracted from the composite sedimentary record and were not part of the age model for the analyzed sequence (Fig. 2).

4.2. Chronostratigraphy

The radiocarbon chronology of the composite section was established using two samples containing terrestrial leaf remains that were collected from the short core (4WS05-S1), and four radiocarbon dates obtained formerly from the long piston core (4WS00-1P) (Table 2; Fig. 3; Schnellmann, 2004). One radiocarbon age from a nearby correlated core (4WS00-2P; Fig. 1) has been furthermore plotted in Fig. 3.

The combustion-derived products contained in the sediments of Lake Lucerne were used to date the most recent sediments using the known periods of the ship engine burning types (Fig. 3). Under the light-microscope, some of the particulate emissions produced by the high temperature combustion of oil, coal, or resinous woods have an irregular or spherical morphology with surface appearances ranging from clear and glassy to black metallic (Figs. 4-1a and 2a). However, the fly-ash particles produced by wood or coal and those produced by oil appear relatively similar when viewed through light-microscopy, but changes in the particle morphologies and textures can be distinguished from one another when examined through scanning electron microscopy (SEM) (Griffin and Goldberg, 1979). Indeed, SEM observations demonstrate that the etched, convoluted layer structures between pores (Fig. 4-1b and 1c) are unique to fly-ash particles originating from fuel-oil combustion (Griffin and Goldberg, 1981). In contrast, charcoal from coal and wood burning are characterized by elongate or prismatic particles. Natural and human-induced wood burning can yield carbon particles that resemble those produced from coal burning, but the common morphology is elongate-prismatic with well preserved wood cells (Figs. 4-3a–c) so that these wood-derived particles can be distinguished from others.

Table 2
Radiocarbon (^{14}C) age determination for cores 4WS05-S1, 4WS00-1P, and 4WS00-2P

Core	Depth in record (cm)	Type	Sample number	AMS ^{14}C age (year)	Cal. age BP (year)	Cal. age AD/BC (year)	$\delta^{13}\text{C}$ (‰)
4WS05-S1	53	Leaf	ETH-31562	490 ± 65	545 ± 61	1405 ± 61 AD	-21.9 ± 1.2
4WS05-S1	103	Leaf	ETH-31563	1280 ± 55	1206 ± 62	744 ± 62 AD	-25.9 ± 1.2
4WS00-1P	164	Leaf	UZ-5038	2100 ± 50	2079 ± 64	129 ± 64 BC	-28.4 ± 1.2
4WS00-1P	214	Leaf	UZ-4571	2440 ± 50	2533 ± 128	583 ± 128 BC	-20.6 ± 1.2
4WS00-1P	374	Leaf	UZ-5039	4400 ± 55	5043 ± 136	3093 ± 136 BC	-25.2 ± 1.2
4WS00-1P	541	Wood	UZ-4949	6150 ± 65	7054 ± 90	5104 ± 90 BC	-21.7 ± 1.2
4WS00-2P	210	Leaf	UZ-4572	2230 ± 60	2240 ± 72	290 ± 72	-22.3 ± 1.2

Pretreatment of the samples and graphitization were carried out at the University of Zürich and ETH, Zürich. ^{14}C analyses were made at the AMS Radiocarbon Laboratory at the ETH/PSI facility at Hönggerberg, Zürich (Bonani et al., 1987). The ^{14}C ages were calculated following the convention of Stuiver and Polach (1977) and calibrated (1 sigma range) using CalPal calibration program (<http://www.calpal.de>) (version CalPal 2005 SFCP) with INTCAL04 (March 2005, Reimer et al., 2004) and Fairbanks et al. (2005) data set.

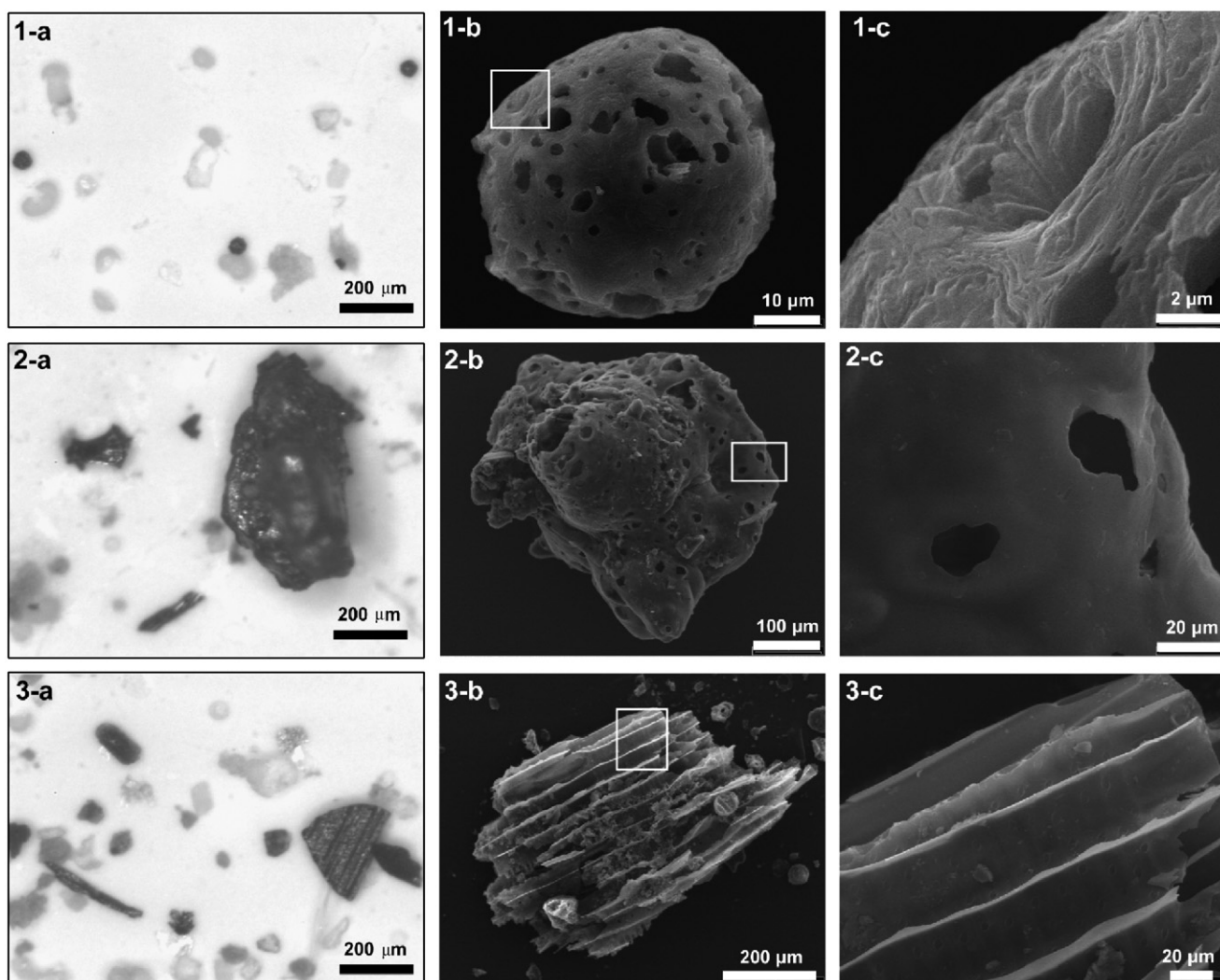


Fig. 4. Microscope photographs from core 4WS05-S1 showing (1) Particles from the burning of oil (from a depth of 12 cm) through incident-light microscope (1-a), single cenosphere through scanning electron microscope (1-b) and the square outlined in 1-b at higher magnification (1-c). (2) Particles from the burning of coal (from a depth of 18 cm) through incident-light microscope (2-a), single cenosphere through scanning electron microscope (2-b) and the square outlined in 2-b at higher magnification (2-c). (3) Particles from the burning of wood (from a depth of 22 cm) through incident-light microscope (3-a), through scanning electron microscope (3-b) and the square outlined in 3-b at higher magnification (3-c).

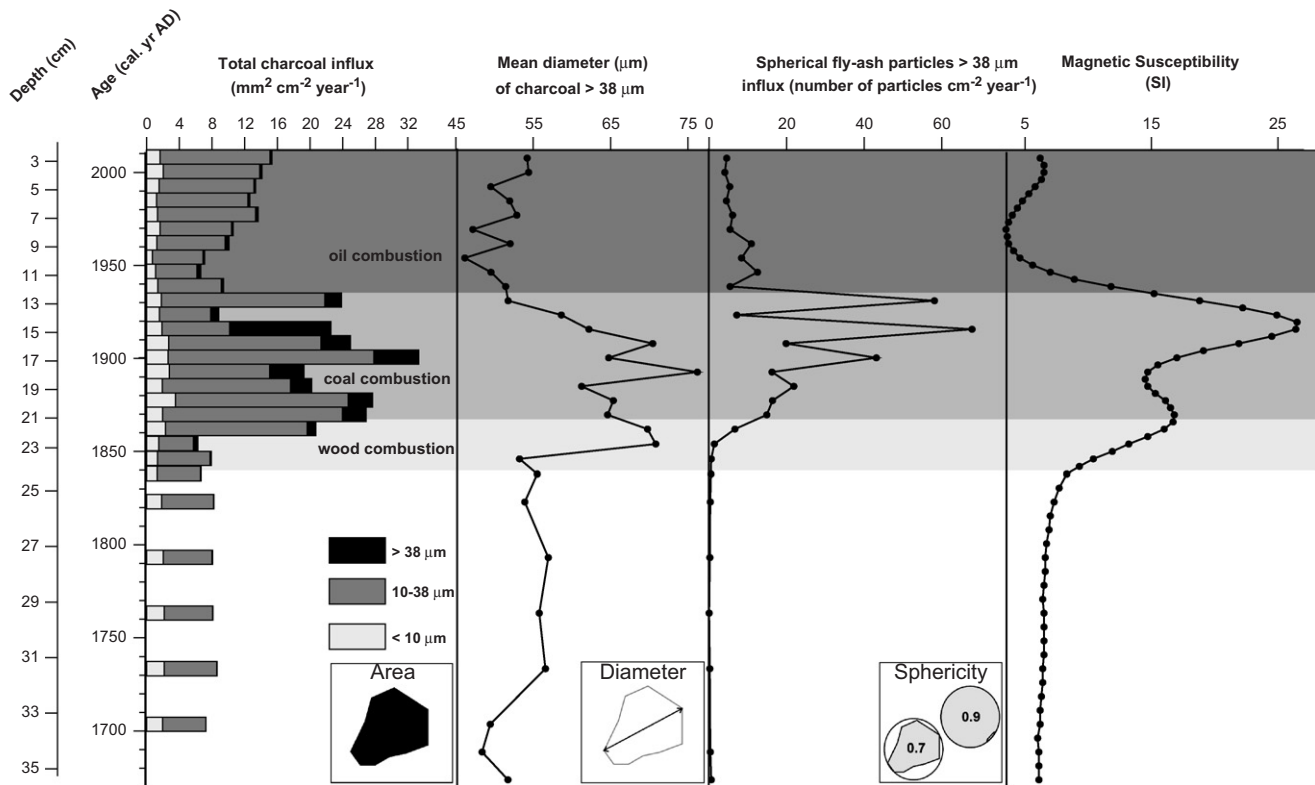


Fig. 5. ca 300 year-record of charcoal influx (<10, 10–38 and >63 μm) from Lake Lucerne, mean diameter of the coarse charcoal fraction, spherical fly-ash particle influx, and magnetic susceptibility.

In the topmost section, the charcoal and spherical fly-ash particles influxes, as well as the magnetic susceptibility and the mean size of the coarse charcoals, increase above a sediment depth of ca 24 cm (Fig. 5). This event is accompanied by an increase in wood residues of combustion (Fig. 4-3), which marks the advent of high-temperature wood burning in the area. The associated age is AD 1838, when the first steamship line was established on Lake Lucerne (Table 1). The successive burning of coal produced high amounts of sedimentary slag particles (Behbehani et al., 1986), and also magnetic and carbonaceous coal fly-ash particles. Using SEM, fly-ash particles from coal burning have been identified in Lake Lucerne sediments showing spheroidal shaped particles with smooth homogeneous surfaces between the pores (Figs. 4-2b and c). These observations demonstrate that the peak in spherical fly-ash particles and magnetic susceptibility at 21 cm core-depth (Fig. 5) coincides with the arrival of the coal-driven ships that were established on Lake Lucerne AD 1862. The first appearance of oil particle morphology at 12 cm (Figs. 4-1b and c) suggests an age of AD 1931, coinciding with the first use of diesel engines and smaller particles emissions in Lake Lucerne (Fig. 5).

4.3. Prehistoric and historic biomass burning record

The distribution of the combustion-derived products is presented in Fig. 6 for the small (<38 μm) and the coarse

(>38 μm) charcoal size-classes. The results are expressed in charcoal area per gram of dry sediment (mm^2g^{-1}) and converted in charcoal influx (charcoal area \times sedimentation rate \times density; $\text{mm}^2\text{cm}^{-2}\text{yr}^{-1}$). For the calculation, the value for density of the sediment was 1.31gcm^{-3} (as obtained from the averaged multisensor core-logger data), and the sedimentation rate was 0.08cm yr^{-1} (as given by the averaged age model, Fig. 3).

The coarse charcoal deposition was lowest between 7150 and 5800 cal. BP (5200–3850 BC), not exceeding $0.04\text{mm}^2\text{cm}^{-2}\text{yr}^{-1}$, while it increased abruptly at ca 5700 and 5550 cal. BP (ca 3750 and 3600 BC) and reached its maximum prehistoric values at ca 5500 cal. BP (ca 3550 BC) ($0.29\text{mm}^2\text{cm}^{-2}\text{yr}^{-1}$). This great increase in the coarse particles influx occurred at the end of the Middle Neolithic, and charcoal particles remained abundant until the beginning of the Younger Neolithic, at ca 5200 cal. BP (ca 3250 BC). During the Younger Neolithic, coarse charcoal influx stayed relatively low, except relatively elevated values between ca 4900 and 4500 cal. BP (ca 2950 and 2550 BC). A peak of similar amplitude (ca $0.07\text{mm}^2\text{cm}^{-2}\text{yr}^{-1}$) occurred during the Early Bronze Age at ca 3950 cal. BP (ca 2000 BC), while the transition with the Late Bronze Age at ca 3300 cal. BP (ca 1350 BC) was marked by an important peak of coarse charcoal influx ($0.19\text{mm}^2\text{cm}^{-2}\text{yr}^{-1}$). Significant coarse charcoal influx was present throughout the Bronze and Iron Ages, and a major peak is centered on the transition between the Early

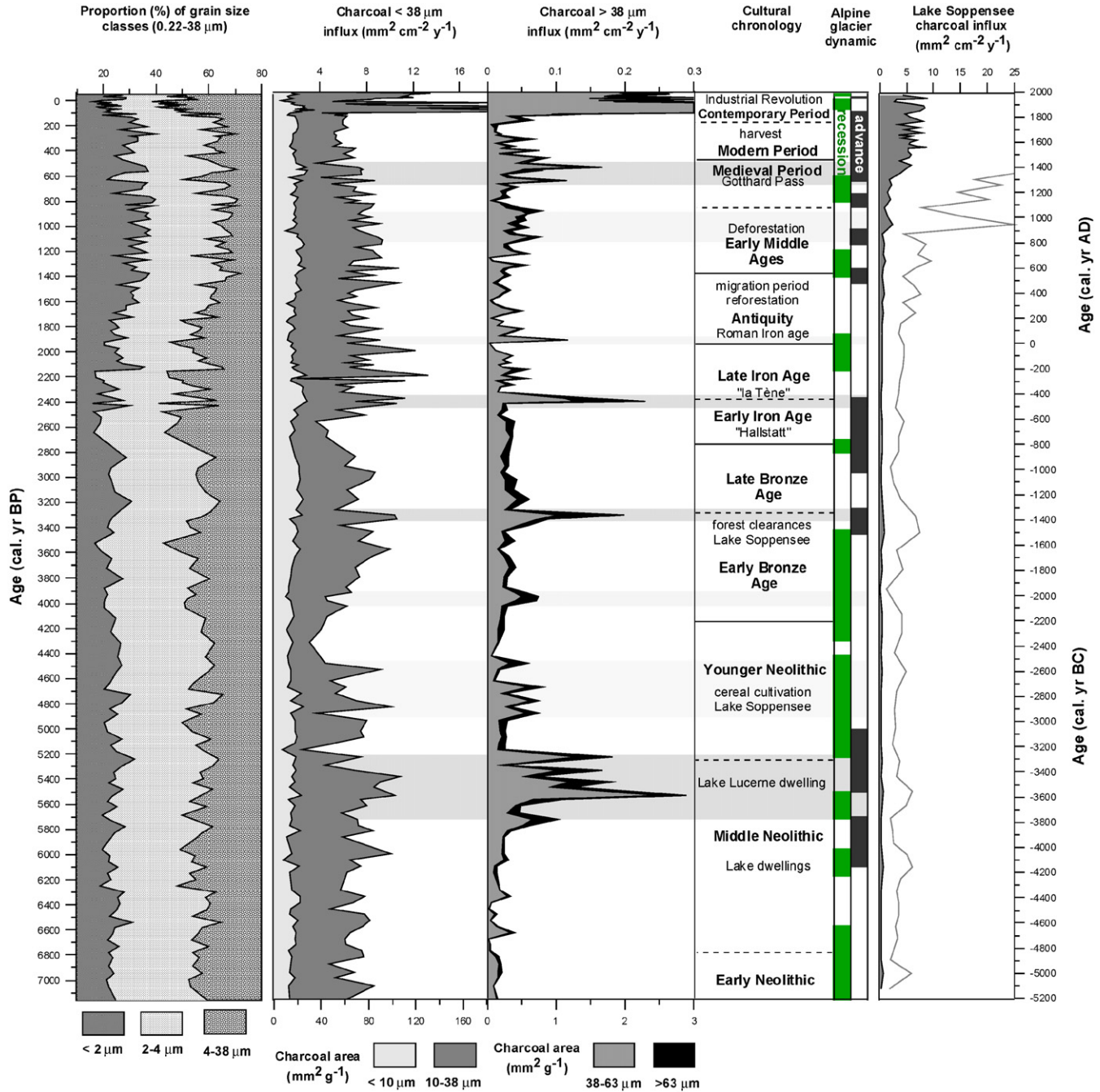


Fig. 6. Proportion (%) of the grain size classes from the fraction 0.22–38 μm . Charcoal area and charcoal influx records from Lake Lucerne, compared with the cultural chronology, with the Alpine glacier dynamic (Hormes et al., 2001; Holzhauser et al. 2005; Joerin et al., 2006), with the Soppensee charcoal record from Tinner et al. (2005). To allow a better overview for small values, the charcoal influx values from Soppensee are 10 times exaggerated for the empty gray line, while the gray full polygon curves gives the original values.

and Late Iron Age at ca 2400 cal. BP (ca 450 BC; $0.23 \text{ mm}^2 \text{ cm}^{-2} \text{ yr}^{-1}$). Although these prehistoric peaks of coarse charcoal were associated with abundant small charcoal deposition, the distribution of the smaller particles showed relatively high values throughout the entire record (ca $8 \text{ mm}^2 \text{ cm}^{-2} \text{ yr}^{-1}$), but important drops around 5200 cal. BP (3250 BC), 4500–4100 cal. BP (2550–2150 JC), 2800–2500 cal. BP (850–550 JC), 2200 cal. BP (250 JC), and 400–200 cal. BP (AD 1550–1750). This last decrease is also

observed in the coarse charcoal abundance. After relatively high charcoal values during the Roman period (15 BC–AD 375), a general trend towards increasing charcoal influx can be observed during the past 2000 years, except of a drop after ca AD 1100, during the Medieval Warm Period (ca AD 1000–1300; Hughes and Diaz, 1994), while the coarse charcoal abundance re-increased between ca AD 1300 and 1550, during the Little Ice Age (ca AD 1200–1850; Grove, 1987).

4.4. Contemporary fossil-fuel combustion record

During the Contemporary Period, the coarse charcoal influx increased by a factor 10 from AD 1868 to 1931 with the great occurrence of coal particles from steamships (Fig. 5). Maximum combustion-derived products deposition occurred around AD 1900 for the small ($27.8 \text{ mm}^2 \text{ cm}^{-2} \text{ yr}^{-1}$) and coarse ($5.5 \text{ mm}^2 \text{ cm}^{-2} \text{ yr}^{-1}$) fractions (Fig. 5). The Lake Lucerne sediment record shows that the coal-combustion products emitted by the steam vessels were almost equivalent to the charcoal influx before the industrial revolution.

5. Discussion

5.1. Charcoal record interpretation

Subtracting the background from charcoal time series is a prerequisite to interpret charcoal peaks as fire episodes and to calculate fire frequencies (Thevenon et al., 2003; Asselin and Payette, 2005; Higuera et al., 2005; Whitlock et al., 2006; Carcaillet, 2007). The charcoal-size distribution of Lake Lucerne record shows that the background signal is mostly contained in the charcoal fraction $< 38 \mu\text{m}$ (Fig. 6). Indeed, the small charcoal influx exhibits relatively similar variations as those observed in the clay-size mineral distribution (grain size $< 4 \mu\text{m}$). This result suggests that in the pre-industrial period, (1) the detrital μm -charcoal degradation products may constitute the main source of charcoal particles, and (2) the small charcoal transport to Lake Lucerne sediment is primarily linked to the surface runoff from the large catchment area of Lake Lucerne. By contrast, the coarse charcoal background is relatively low, and sharp peaks of coarse charcoal occur independently from the grain-size distribution profiles (Fig. 6). Although the contribution of reworked coarse charcoal should not be definitively ruled out, we postulate that the coarse charcoal peaks may rather reflect of major fire episodes, because (i) the four identified silty horizons have been subtracted from the composite sedimentary record and the charcoal horizons are not coeval with some particular sedimentological and petrophysical features (grain size, magnetic susceptibility, or density peaks), (ii) the charcoal horizons contain relatively large ($> 63 \mu\text{m}$) and well preserved charcoal, excluding the remobilization of fossil particles, and (iii) these charcoal peaks coincide with some major regional socio-cultural changes and with the regional fire history (Fig. 6 and discussion below).

5.2. Biomass burning and fossil fuel reconstruction

The coarse charcoal influx indicates that regional fire activity increased dramatically from ca 5700 to 5200 cal. BP (3550–3250 BC). The highest charcoal peak at 5500 cal. BP (3350 BC) coincides remarkably with the Neolithic Lake Lucerne shore settlement site (i.e. lake dwelling) that has been recently discovered on a submerged platform ca 8 m

below the present day lake-level, and dated at ca 5450 cal. BP (3500 BC) (Hügi, 2006). Moreover, these results also fit with the marked charcoal influx peak recorded at 5500–5400 cal. BP from Soppensee (Fig. 6) and Lobsigensee, and with the earliest phase of introduction of agriculture in Central Europe (Tinner et al., 2005). The subsequent increases in the coarse charcoal record between ca 4900 and 4500 cal. BP (2950–2550 BC), correspond to the increased occurrence of anthropogenic indicator pollen (e.g. *Cerealia*, *Plantago lanceolata*) between 5000 and 4500 BP (3050–2550 BC) in the sediment record from Soppensee (Lotter, 1999), a lake located only ca 17 km NE of Lucerne. These observations thus strongly support the assumption of an increased fire activity linked to local changes in land-use during the Younger Neolithic, when arable and pastoral farming expanded over almost entire Central Europe. This could be also the case later during the Bronze Age: Relatively high coarse charcoal values are registered in Lake Lucerne sediments at ca 3950 cal. BP (2000 BC) and especially within the transition with the Late Bronze Age at ca 3300 cal. BP (ca 1350 BC), also coinciding with a charcoal peak in Soppensee (Fig. 6). In fact, at Soppensee, forest clearances and local settlements are preponderant between ca 3800 and 3000 cal. BP (ca 1850–1050 BC) (Lotter, 2001). In the Lake Lucerne record, a high peak of coarse charcoal also marks the transition between the Early Iron Age (i.e. the Hallstatt Culture), and the Late Iron Age (i.e. La Tène), at ca 2400 cal. BP (ca 450 BC) (Fig. 6). We note that this event could also be ca 200 years younger, taking into account the uncertainty of the age model used for this part of the core (i.e. considering an alternate date from a nearby correlated core, 4WS00-2P; Fig. 3). However, a ca 2400 cal. BP fire episode strikingly matches with (i) the first major forest clearances that took place during the Iron Age around Soppensee, ca 2500 years ago (550 BC) (Lotter 2001), (ii) the big fire event recorded at ca 2500 cal. BP in lakes Lobsigen, Muzzano, and Origgio (Tinner et al., 2005), and (iii) the technological progress associated to the beginning of the Late Iron Age in Switzerland. Indeed, the archeological site of La Tène (on the northern edge of Lake Neuchatel), which is a representative site for the Celtic development and expansion, gave its name to the cultures of the Late Iron Age in Europe, from 2400 cal. BP (450 BC) to the Roman conquest at 2050 cal. BP (1st century BC).

The coarse charcoal record from Lake Lucerne contains a sharp peak at the beginning of the Roman period (15 BC–AD 375), while low fire activity is inferred during the Migration period (AD 375–534), which is known as a period of abandonment and reforestation in Northwest Europe (Berglund, 2003). Coarse charcoal influx tends to increase during the Early Middle Age (AD 534–1050), while lower values occur during the first part of the Medieval Period (AD 1050–1500). The local fire activity finally re-increases after the opening of the Gotthard Pass (AD 1230) together with the socio-economic development of the Lake Lucerne surroundings. Despite high charcoal

values at the beginning of the Modern Period (AD 1501–1798) the subsequent times show a relative decrease in charcoal influx, especially between AD 1660 and 1730. A lower biomass burning activity during the end of the Little Ice Age could be linked to the reduced socio-economic activity in Central Europe, as known by the documented conflicts, diseases, and harvest-periods (Brazdil et al., 2005).

For the Contemporary Period (AD 1803–today), the dramatic increase in charcoal influx and magnetic susceptibility resulted from the development of the steamboat traffic on Lake Lucerne and the associated high combustion of wood and fossil-fuel (Figs. 5 and 6). In fact, the great peak of coal-combustion products during the nineteenth-century in Lake Lucerne sediments precisely marks the beginning of the Industrial Revolution in this part of the Swiss Plateau and its large impact on the environment.

It is interesting to note that most of the reported fire episodes, at ca 5700–5200, 4900–4500, 3950, 3300, 2400, 1900, 1100–900, and 700–500 cal. BP (see details above), occurred during periods of climate cooling in the Northern Hemisphere (Von Grafenstein et al., 1998; D'Arrigo et al., 2006). Furthermore, the largest fire episodes (ca 5500, 3300, 2400, and 530 cal. BP) took place during regional cold phases (Magny and Haas, 2004; Haas et al., 2006) and glacier advances (Hormes et al., 2001; Holzhauser et al., 2005; Joerin et al., 2006) (Fig. 6), which are linked to the impact of general winter cooling and increase in summer moisture (Holzhauser et al., 2005). The positive correlation between human impact and climate deterioration observed from our results implies that human migration and settlements patterns on the Swiss Plateau could have been at least partially triggered by climatic unfavorable environmental conditions (Berglund, 2003; Zolitschka et al., 2003).

6. Conclusion

The newly developed automated optical method allows the complete and reproducible quantification of the combustion-derived products stored in Lake Lucerne sediments. Moreover, the combined analysis of the charcoal morphology by optical and electronic microscopes enables us to decipher the specific products of high-temperature and fossil-fuel combustion (black fly-ash particles), providing useful chronological markers for the recent deposits, as well as a record of the fossil-fuel combustion impact. In particular, the coal combustion produced large amount of inorganic ash spheres, increasing the magnetic susceptibility of the sediments.

Although the majority of the small charcoal recruitment in the pre-industrial period appears to be primarily linked to runoff from the large lake basin, the coarse charcoal distribution presents an independent signal that correlates well with the documented regional fire history. Moreover, the inferred major fire episodes are also strikingly synchronous with the newly discovered Neolithic settle-

ment along Lake Lucerne (5700–5550 cal. BP, 3750–3600 BC), with the local development of agricultural practices (4900–4500 cal. BP, 2950–2550 BC) during the Neolithic period, with the innovations in the metallurgy during the Bronze Age (3300 cal. BP, 1350 BC) and the Iron Age (2400 cal. BP, 450 BC), and with the onset of the steamer traffic during the industrialization (from AD 1838).

The prehistoric periods of human impact in Central Switzerland indicate a striking synchronicity not only with the major documented technical, land-use, and socio-economics changes, but also with periods of regional climate cooling and unstable environmental conditions. Such unfavorable conditions probably influenced human settlement patterns in the Swiss Plateau together with land-use changes or technological and social innovations. A comparison between supplementary sites would give additional spatiotemporal information about cultural innovations and a better understanding of the major European land-use changes related to climatic and/or socio-economic global changes. Furthermore, it may enable us to quantify, how far the socio-economic aspects contributed to regional-scale environmental change.

Acknowledgments

This project was funded by the French Ministry of Foreign Affairs (postdoctoral Lavoisier grant) and received additional support from ETH Zurich and Swiss National Science Foundation. We thank H. Thierstein for providing access to the micropaleontology laboratory of the ETH of Zurich, and H. S. Lan for the SEM sessions. We are grateful to the Limnogeology group from the ETH Zurich, in particular to M. Schnellmann for various discussions and core data, M. Strasser and R. Hofmann for the coring on Lake Lucerne, S. Girardclos for the core logging data, E. Chapron for assistance with the grain-size analyzer, and U. Gerber for core photography. The Eawag Limnologic Research Center in Kastanienbaum provided logistic support for coring operations. We acknowledge L. Beaufort for allowing the utilization of the automated transmitted-light microscope (CEREGE/CNRS Aix-en-Provence). We are thankful to W. Tinner and N. Roberts for many constructive comments and suggestions on this manuscript.

References

- Andreae, M.O., 1991. Biomass burning: its history, use, and distribution and its impact on environmental quality and global climate. In: Levine, J.S. (Ed.), *Global Biomass Burning: Atmospheric, Climatic, and Biospheric Implications*. The MIT Press, Cambridge, MA, pp. 3–21.
- Asselin, H., Payette, S., 2005. Detecting local-scale fire episodes on pollen slides. *Review of Palaeobotany and Palynology* 137, 31–40.
- Behbehani, A.R., Miiller, J., Schmidt, R., Schneider, J., Schroder, H.-G., Srackebrock, I., Sturm, M., 1986. Sediments and sedimentary history of Lake Attersee (Salzkammergut, Austria). *Hydrobiologia* 143, 233–246.
- Berglund, B.E., 2003. Human impact and climate changes—synchronous events and a causal link? *Quaternary International* 105, 7–12.

- Bonani, G., Beer, J., Hofmann, H.-J., Synal, H.-A., Wöflfi, W., Pfeleiderer, C., Kromer, B., Junghaus, C., Münnich, K.O., 1987. Fractionation, precision and accuracy in ^{14}C and ^{13}C measurements. In: Gove, H.E., Litherland, A.E., Elmore, D. (Eds.), *Proceedings of the 4th International Conference on Accelerator Mass Spectrometry*. Nuclear Instruments and Methods in Physics Research B29, pp. 87–90.
- Brazdil, R., Pfister, C., Wanner, H., von Storch, H., Luterbacher, J., 2005. Historical climatology in Europe—the state of the art. *Climatic Change* 70 (3), 363–430.
- Carcaillet, C., 2007. Charred particle analysis. *Paleobotany*, 1582–1593.
- Carcaillet, C., Almquist, H., Asnong, H., Bradshaw, R.H.W., Carrion, J.S., Gaillard, M.J., et al., 2002. Holocene biomass burning and global dynamics of the carbon cycle. *Chemosphere* 49, 845–863.
- Clark, J.S., Patterson, W.A., 1997. Background and local charcoal in sediments: scales of fire evidence in the paleorecord. In: Clark, J.S., Cachier, H., Goldammer, J.G., Stocks, B. (Eds.), *Sediment records of biomass burning and global change*. NATO, Berlin, pp. 23–48.
- Clark, J.S., Hussey, T.C., Royall, P.D., 1996. Presettlement analogs for Quaternary fire regimes in eastern North America. *Journal of Paleolimnology* 16, 79–96.
- Currie, L.A., et al., 2002. A critical evaluation of interlaboratory data on total, elemental, and isotopic carbon in the carbonaceous particle reference material NIST SRM 1649a. *Journal of Research of the National Institute of Standards and Technology* 107, 279–298.
- D'Arrigo, R., Wilson, R., Jacoby, G., 2006. On the long-term context for late twentieth century warming. *Journal of Geophysical Research—Atmospheres* 111, D03103.
- Fairbanks, R.G., Mortlock, R.A., Chiu, T.-C., Cao, L., Kaplan, A., Guilderson, T.P., Fairbanks, T.W., Bloom, A.L., 2005. Marine radiocarbon calibration curve spanning 10,000–50,000 years BP based on paired $^{230}\text{Th}/^{234}\text{U}/^{238}\text{U}$ and ^{14}C dates on Pristine Corals. *Quaternary Science Reviews* 24, 1781–1796.
- Francus, P., Bradley, R., Thurow, J., 2004. An introduction to image analysis, sediments and paleoenvironments. In: Francus, P. (Ed.), *Image Analysis, Sediments and Paleoenvironments*. Springer, Dordrecht, The Netherlands, pp. 1–7.
- Gälman, V., Petterson, G., Renberg, I., 2006. A comparison of Sediment Varves (1950–2003 AD) in two adjacent lakes in Northern Sweden. *Journal of Paleolimnology* 35, 837–853.
- Girardclos, S., Schmidt, O.T., Sturm, M., Ariztegui, D., Pugin, A., Anselmetti, F.S., 2007. The 1996 AD delta collapse and large turbidite in Lake Brienz. *Marine Geology* 241, 137–154.
- Goldberg, E.D., Hodge, V.F., Griffin, J.J., Koide, M., 1981. Impact of fossil-fuel combustion on the sediments of Lake Michigan. *Environmental Science and Technology* 15, 466–471.
- Griffin, J.J., Goldberg, E.D., 1979. Morphologies and origin of elemental carbon in the environment. *Science* 206, 563–565.
- Griffin, J.J., Goldberg, E.D., 1981. Sphericity as a characteristic of solids from fossil-fuel burning in a Lake Michigan sediment. *Geochimica et Cosmochimica Acta* 45, 763–769.
- Grove, J., 1987. *The Little Ice Age*. Methuen, London, 498p.
- Haas, J.N., Richoz, I., Tinner, W., Wick, L., 2006. Synchronous Holocene climatic oscillations recorded on the Swiss Plateau and at timberline in the Alps. *The Holocene* 8 (3), 301–309.
- Higuera, P.E., Sprugel, D.G., Brubaker, L.B., 2005. Reconstructing fire regimes with charcoal from small-hollow sediments: a calibration with tree-ring records of fire. *The Holocene* 15, 238–251.
- Holzhauser, H., Magny, M., Zumbuhl, H.J., 2005. Glacier and lake-level variations in west-central Europe over the last 3500 years. *The Holocene* 15, 789–801.
- Hormes, A., Müller, B.U., Schlüchter, C., 2001. The Alps with little ice: evidence for eight Holocene phases of reduced glacier extent in the Central Swiss Alps. *The Holocene* 11, 255–265.
- Hughes, M.K., Diaz, H.F., 1994. Was there a “Medieval Warm Period” and if so, where and when? *Climatic Change* 26, 109–142.
- Hügi, U., 2006. Stansstad NW-Kehrsiten: neolithische Seefersiedlungen am Alpennordrand. *Jahrbuch der Schweizerischen Gesellschaft für Ur- und Frühgeschichte* 89, 7–23.
- Joerin, U.E., Stocker, T.F., Schlüchter, C., 2006. Multicentury glacier fluctuations in the Swiss Alps during the Holocene. *The Holocene* 16 (5), 697–704.
- Kralovec, A.C., Christensen, E.R., Van Camp, R.P., 2002. Fossil fuel and wood combustion as recorded by carbon particles in Lake Erie sediments 1850–1998. *Environmental Science and Technology* 36 (7), 1405–1413.
- Kuhlbusch, T.A.J., Crutzen, P.J., 1995. Toward a global estimate of black carbon in residues of vegetation fires representing a sink of atmospheric CO_2 and a source O_2 . *Global Biogeochemical Cycles* 9, 491–501.
- Lotter, A.F., 1999. Lateglacial and Holocene vegetation history and dynamics as evidenced by pollen and plant macrofossil analyses in annually laminated sediments from Soppensee (Central Switzerland). *Vegetation History and Archaeobotany* 8, 165–184.
- Lotter, A.F., 2001. The palaeolimnology of Soppensee (Central Switzerland), as evidenced by diatom, pollen, and fossil-pigment analyses. *Journal of Paleolimnology* 25, 65–79.
- Magny, M., Haas, J.N., 2004. A major widespread climatic change around 5300 cal. yr BP at the time of the Alpine Iceman. *Journal of Quaternary Science* 19 (5), 423–430.
- Masiello, C.A., 2004. New directions in black carbon organic geochemistry. *Marine Chemistry* 92, 201–213.
- Odgaard, B.V., 1994. The use of spheroidal carbonaceous particles for quantifying modern pollen deposition rates. *Review of Palaeobotany and Palynology* 82, 157–164.
- Reimer, P.J., Baillie, M.G.L., Bard, E., Bayliss, A., Beck, J.W., Blackwell, P.G., Buck, C.E., Burr, G.S., Cutler, K.B., Damon, P.E., Edwards, R.L., Fairbanks, R.G., Friedrich, M., Guilderson, T.P., Herring, C., Hughen, K.A., Kromer, B., McCormac, F.G., Manning, S.W., Ramsey, C.B., Reimer, P.J., Reimer, R.W., Remmele, S., Southon, J.R., Stuiver, M., Talamo, S., Taylor, F.W., van der Plicht, J., Weyhenmeyer, C.E., 2004. IntCal04 Terrestrial radiocarbon age calibration, 0–26 cal. ka BP. *Radiocarbon* 46 (3), 1029–1058.
- Rose, N.L., Harlock, S., Appleby, P.G., Battarbee, R.W., 1995. Dating of recent lake sediments in the United Kingdom and Ireland using spheroidal carbonaceous particle (SCP) concentration. *The Holocene* 5, 328–335.
- Schnellmann, M., 2004. Late quaternary mass movements in a Perialpine Lake (Lake Lucerne, Switzerland)—sedimentary processes, natural hazards and paleoseismic reconstructions. Ph.D. Thesis, ETH Zürich, Zürich, 132pp.
- Schnellmann, M., Anselmetti, F.S., Giardini, D., McKenzie, J.A., 2006. 15,000 years of mass-movement history in Lake Lucerne: implications for seismic and tsunami hazard. *Eclogae Geologicae Helveticae* 99 (3), 409–428.
- Seelos, K., Sirocko, F., 2005. RADIUS-rapid particle analysis of digital images by ultra-high-resolution scanning of thin sections. *Sedimentology* 52, 669–681.
- Strasser, M., Stegmann, S., Bussmann, F., Anselmetti, F.S., Rick, B., Kopf, A., 2007. Quantifying subaqueous slope stability during seismic shaking: Lake Lucerne as model for ocean margins. *Marine Geology* 240, 77–97.
- Stuiver, M., Polach, H.A., 1977. Discussion: reporting of ^{14}C data. *Radiocarbon* 19 (3), 355–363.
- Suman, D.O., Kuhlbusch, T.A.J., Lim, B., 1997. Marine sediments: a reservoir for black carbon and their use as spatial and temporal records of combustion. In: Clark, J.S., Cachier, H., Goldammer, J.G., Stocks, B. (Eds.), *NATO ASI Series I: Global Environmental Change*. Springer, Berlin, Heidelberg, New York, pp. 271–293.
- Thevenon, F., Williamson, D., Vincens, A., Taieb, M., Merdaci, O., Decobert, M., Buchet, G., 2003. A Late Holocene charcoal record from Lake Masoko, SW Tanzania: climatic and anthropologic implications. *The Holocene* 13 (5), 785–792.
- Thevenon, F., Bard, E., Williamson, D., Beaufort, L., 2004. A biomass burning record from the West Equatorial Pacific over the last 360 ka: methodological, climatic and anthropic implications. *Palaeogeography, Palaeoclimatology, Palaeoecology* 213, 83–99.

- Thevenon, F., Williamson, D., Bard, E., Anselmetti, F., Cachier, H., Beaufort, L., in press. Combining charcoal and black carbon analysis in natural archives: implications for past fire regimes, the pyrogenic carbon cycle, and the human–climate interactions. *Global and Planetary Change*.
- Tinner, W., Hubschmid, P., Wehrli, M., Ammann, B., Conedera, M., 1999. Long-term forest fire ecology and dynamics in southern Switzerland. *Journal of Ecology* 87, 273–289.
- Tinner, W., Conedera, M., Ammann, B., Lotter, A.F., 2005. Fire ecology north and south of the Alps since the last ice age. *The Holocene* 15 (8), 1214–1226.
- Tinner, W., Hofstetter, S., Zeugin, F., Conedera, M., Wohlgemuth, T., Zimmermann, L., Zweifel, R., 2006. Long-distance transport of macroscopic charcoal by an intensive crown fire in the Swiss Alps—implications for fire history reconstruction. *The Holocene* 16 (2), 287–292.
- Turner, R., Roberts, N. and Kelly, A., in press 2007. A critical assessment of the methods used to extract and experimental comparison of microscopic charcoal from lake sediments. In: Fiorentino, G., Magri, D. (Eds.), *Charcoal from the Past: Cultural and Palaeoenvironmental Implications*. Proceedings of the Third International Meeting of Anthracology, Cavallino (Lecce), June 2004. BAR International Series, Archaeopress, Oxford, UK.
- Umbanhowar Jr., C.E., McGrath, M.J., 1998. Experimental production and analysis of microscopic charcoal from wood, leaves and grasses. *The Holocene* 8, 341–346.
- Von Grafenstein, U., Erlenkeuser, H., Müller, J., Jouzel, J., Johnsen, S., 1998. The short cold period 8200 years ago documented in oxygen isotope records of precipitation in Europe and Greenland. *Climate Dynamics* 14, 73–81.
- Whitlock, C., Bianchi, M.M., Bartlein, P.J., Markgraf, V., Walsh, M., Marlon, J.M., McCoy, N., 2006. Postglacial vegetation, climate, and fire history along the east side of the Andes (lat 41–42.5 S), Argentina. *Quaternary Research* 66, 187–201.
- Wik, M., Renberg, I., 1996. Environmental records of carbonaceous fly-ash particles from fossil-fuel combustion. *Journal of Paleolimnology* 15, 193–206.
- Zolitschka, B., Behre, K.E., Schneider, J., 2003. Human and climatic impact on the environment as derived from colluvial, fluvial and lacustrine archives: examples from the Bronze Age to the Migration period, Germany. *Quaternary Science Reviews* 22, 81–100.